Scilight

Complex Systems Stability & Control
https://www.sciltp.com/journals/cssc

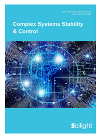

Article

Bifurcations of a Fractional-Order Inertial Neural Network: Neutral-Type Delays

Chengdai Huang [1,*], Huimeng Chen [1], Jinde Cao [2] and Heng Liu [3]

[1] School of Mathematics and Statistics, Xinyang Normal University, Xinyang 464000, China
[2] School of Mathematics, Southeast University, Nanjing 210096, China
[3] School of Mathematical Sciences, Guangxi Minzu University, Nanning 530006, China
[*] Correspondence: huangchengdai@163.com or chdhuang1986@xynu.edu.cn

How To Cite: Huang, C.; Chen, H.; Cao, J.; et al. Bifurcations of a Fractional-Order Inertial Neural Network: Neutral-Type Delays. *Complex Systems Stability & Control* **2026**, *2*(3), 7. https://doi.org/10.53941/cssc.2026.100018

Received: 23 April 2026
Revised: 5 June 2026
Accepted: 9 June 2026
Published: 20 July 2026

Abstract: The bifurcation problems of the four-neuron fractional-order neutral-type inertial neural network (FONTINN) are examined. We study the dynamic characteristics of the system by viewing time delay as the bifurcation parameter. By exploiting the Cramer's rule, the results with regard to delay-dependent bifurcations are obtained. Experimental results show that when time delay is less than the critical value, the stability of system can be well maintained, and Hopf bifurcation occurs when time delay exceeds its critical value. Furthermore, it also reveals that fractional orders are instrumental in ameliorating the stability of systems in comparison with the traditional integer-order models. The correctness of the discovered theories is ultimately verified through numerical experiments.

Keywords: stability; hopf bifurcation; inertia terms; fractional-order neutral-type neural network

1. Introduction

Fractional calculus has recently developed a hot topic and numerous applications have been spotted concerning physics and engineering [1–3]. As a matter of fact, a considerable number of studies have shown that incorporating fractional calculus into dynamic systems can enhance the ability to characterize, design, and control these systems. Artificial neural network, abbreviated as neural network, is a mathematical model that simulates the processing mechanism of the human brain's nervous system for complex information, composed of a large number of interconnected neurons. This model has high fault tolerance [4], intelligence [5], data fusion [6], and adaptive processing capabilities [7]. It is an interdisciplinary field involving multiple fields such as neuroscience, cognitive science, artificial intelligence, and computer science [8–11]. It has a high degree of nonlinearity, which can improve fault tolerance and storage capacity, and can handle nonlinear relationships and complex patterns. In the theoretical research of neural networks, nonlinear dynamics such as stability, bifurcation, and chaos are important components. The research on neural networks not only helps us understand the mathematical theoretical basis of neural networks, but also provides great assistance for the development, design, and application of neural networks. Currently, neural networks have been successfully applied in research areas such as fault diagnosis [12], combinatorial optimization [13], and medicine [14].

The neural networks that are usually described by using first-order differential equations [15, 16]. Inertial neural networks are special neural networks and characterized by second-order differential equations. They have received much attention in recent years, and their stability, bifurcation, and chaos phenomena have become important research objects. The inertial neural network models contain first and second derivative terms of the system state, therefore they have more complex dynamic characteristics. Research demonstrated that for neural networks, the introduction of inertia terms can more accurately characterize their dynamic characteristics [17], and can be further applied to chaos and bifurcation control [18]. At present, many important achievements have been made in the stability and bifurcation of inertial neural networks [19–21]. In [22], the stability and bifurcation of a Caputo delayed fractional-order BAM neural network and inertia terms were conducted. In [23], the authors combined inertia terms, quaternions, and time-varying discrete and distributed delays into traditional neural networks, and mainly studied the problem of adaptive finite time synchronization for quaternion-valued inertial neural networks with mixed delays. For this reason, an adaptive controller with robustness, simple structure, and low cost was designed. A class of fractional-order generalized reaction-diffusion inertial neural networks were investigated in [24], and their global uniform stability conditions were obtained based on the Lyapunov comparison principle. There are concerns that the inertial terms are carefully incorporated into fractional-order neural networks in this paper in comparison with the developed model in [22]. Therefore, from the perspective of neural network dynamics, the model studied in this paper is closer to the real neural network. This treatment is beneficial for the design and application of neural networks.

In addition, time delay may occur not only in the state of neurons, but also in the time derivative of neuron states. Neutral-type neural networks are models that have time delay in both the neuron state and the time derivative state [25]. At present, research on the dynamics analysis of neutral-type neural networks has also achieved fruitful results. In [26], the authors studied a neutral-type Cohen-Grossberg neural network with mixed time delay, and this was the first article to study the global robust exponential synchronization of neutral-type Cohen-Grossberg neural networks with mixed time delays. There are many types of time delays, such as leakage delay, proportional delay, and neutral delay. In order to comprehensively study neutral-type neural networks, the authors first investigated the stability problems of quaternion neural networks with neutral delay, proportional delay, and leakage delay in [27]. Based on previous research, a novel type of neural network has emerged, namely the NTINNs. This model combines multiple elements, making it more complex and therefore more valuable for research. Previously, scholars have also conducted research on neutral-type inertial neural networks [28–32]. According to the search, there are not many studies on FONTINNs at present, so the research of FONTINNs deserves attention. So, in this article, we will conduct research on FONTINNs to enrich the study of this type of neural network.

Based on the foregoing discussions, the main objective of this article is to examine the stable characteristics of FONTINN. The main contributions of this article are outlined as follows:

(1) Different from [33], inertial terms are introduced into fractional-order neural networks with neutral delays, which is more closely related to real-world scenarios and precisely depict the dynamical behaviors of practical fractional-order neural networks.
(2) Delay-induced bifurcation results of NTINNs are obtained by adopting Cramer's rule. In comparison with traditional method, the developed is neatly utilized to deal with the bifurcations in this article. This treatment directly reduce the computational complexity for analyzing the characteristic equation.
(3) Based on comparative explorations, it detects that the stability performance of NTINNs can be significantly enhanced compared with the corresponding neural networks. Moreover, the onset of bifurcation of NTINNs can be postponed(advanced) by carefully regulating fractional order.

The structure of this article is outlined as follows: in Section 2, some preliminaries on fractional-order derivative. In Section 3, the discussed model is constructed. Section 4 derives the outcomes of bifurcations. The correctness of the results are confirmed by two numerical simulations in Section 5. In Section 6, the conclusions are provided.

2. Principal Conceptions

This section provides some preliminary concepts on fractional calculus.

Definition 1 ([34])**.** *Regarding the Caputo fractional derivative, we define it as*

$$D^{\nu} f(t) = \frac{1}{\Gamma(\alpha-\nu)} \int_0^t (t-s)^{\alpha-\nu-1} f^{(\alpha)}(s) dt,$$

where $\alpha - 1 < \nu \leq \alpha \in Z^{+}$, $\Gamma(\cdot)$ *is the Gamma function.*

By utilizing Laplace transform, we can derive the following equation:

$$L\{D^{\nu} f(t); s\} = s^{\nu} F(s) - \sum_{k=0}^{\alpha-1} s^{\nu-k-1} f^{(k)}(0), \quad \alpha - 1 < \nu \leq \alpha \in Z^{+}.$$

If meet with the zero initial conditions $f^{(k)}(0) = 0$, $k = 0, 1, \ldots, \alpha - 1$, then $L\{D^{\nu} f(t); s\} = s^{\nu} F(s)$.

3. Model Formulation

The following FONTINN is developed in this article.

$$\begin{cases} D^{k_1}V_1(t) = -h_1 D^{k_2}V_1(t) - q_1 V_1(t) + \alpha_{11}F(V_2(t-\iota)) + \mu_1 D^{k_3}V_2(t-\iota), \\ D^{k_1}V_2(t) = -h_2 D^{k_2}V_2(t) - q_2 V_2(t) + \alpha_{21}F(V_3(t-\iota)) + \mu_2 D^{k_3}V_3(t-\iota), \\ D^{k_1}V_3(t) = -h_3 D^{k_2}V_3(t) - q_3 V_3(t) + \alpha_{31}F(V_4(t-\iota)) + \mu_3 D^{k_3}V_4(t-\iota), \\ D^{k_1}V_4(t) = -h_4 D^{k_2}V_4(t) - q_4 V_4(t) + \beta_{11}G(V_1(t-\iota)) + \beta_{12}G(V_2(t-\iota)) + \beta_{13}G(V_3(t-\iota)) \\ \qquad\qquad + \mu_4 D^{k_3}V_1(t-\iota) + \mu_5 D^{k_3}V_2(t-\iota) + \mu_6 D^{k_3}V_3(t-\iota), \end{cases} \tag{1}$$

where $D^{k_1}V_i(t)(i = 1, 2, 3, 4)$ denote the inertial derivative terms; $V_i(t)$ are the state of i-th neuron at time t; k_i express fractional orders; $h_i > 0$ signify the coefficients of damping terms; $q_i > 0$ designate self-regulating parameters; $\alpha_{\upsilon 1}, \beta_{1\upsilon}(\upsilon = 1, 2, 3)$ are connection weights; $\mu_j(j = 1, 2, 3, 4, 5, 6)$ represent the weight of neutral connections; $F(\cdot)$ and $G(\cdot)$ mean nonlinear feedback and activation functions respectively; communication delay is represented by ι.

For the sake of rigor in deduction, we adopt the following assumption.

Hypothesis 1 (H1). $F(\cdot), G(\cdot) \in C(R, R)$, $F(0) = G(0) = 0$.

Remark 1. *The model in this article is an extension of the model in article [33], and inertial derivative terms are added to the model in [33], it is a FONTINN. FONTINNs have the characteristics of past state dependence and inductance effect, which can accurately characterize the reaction process of neurons. Studying the dynamic behavior of FONTINNs under the influence of time delay has important theoretical significance and potential application value.*

Remark 2. *It is not difficult to find that FONTINN (1) can be extended into three models: when $h_i = \mu_j = 0$, the model becomes a fractional-order neural network; when $\mu_j = 0$, it can be transformed into a fractional-order inertial neural network; and finally, when $h_i = 0$, the model becomes a fractional-order neutral-type neural network. We have also achieved many important results in the study of the above models, laying a solid foundation for the research of FONTINN.*

4. Key Results

This section exploits the stability of system (1) with delay ι as the bifurcation parameter.

Apparently, according to Hypothesis 1, the origin is the equilibrium of FONTINN (1).

The linearized equation of FONTINN (1) at the origin can be described as

$$\begin{cases} D^{k_1}V_1(t) = -h_1 D^{k_2}V_1(t) - q_1 V_1(t) + \rho_1(V_2(t-\iota)) + \mu_1 D^{k_3}V_2(t-\iota), \\ D^{k_1}V_2(t) = -h_2 D^{k_2}V_2(t) - q_2 V_2(t) + \rho_2(V_3(t-\iota)) + \mu_2 D^{k_3}V_3(t-\iota), \\ D^{k_1}V_3(t) = -h_3 D^{k_2}V_3(t) - q_3 V_3(t) + \rho_3(V_4(t-\iota)) + \mu_3 D^{k_3}V_4(t-\iota), \\ D^{k_1}V_4(t) = -h_4 D^{k_2}V_4(t) - q_4 V_4(t) + \eta_1(V_1(t-\iota)) + \eta_2(V_2(t-\iota)) + \eta_3(V_3(t-\iota)) \\ \qquad\qquad + \mu_4 D^{k_3}V_1(t-\iota) + \mu_5 D^{k_3}V_2(t-\iota) + \mu_6 D^{k_3}V_3(t-\iota), \end{cases} \tag{2}$$

where $\rho_\upsilon = \alpha_{\upsilon 1}F'(0), \eta_\upsilon = \beta_{1\upsilon}G'(0)(\upsilon = 1, 2, 3)$.

Making use of the theorem in [35], the characteristic equation of system (2) can be obtained as

$$\begin{vmatrix} \ell_{11} & \ell_{12} & \ell_{13} & \ell_{14} \\ \ell_{21} & \ell_{22} & \ell_{23} & \ell_{24} \\ \ell_{31} & \ell_{32} & \ell_{33} & \ell_{34} \\ \ell_{41} & \ell_{42} & \ell_{43} & \ell_{44} \end{vmatrix} = 0,$$

where

$\ell_{11} = s^{k_1} + h_1 s^{k_2} + q_1, \quad \ell_{12} = -\rho_1 e^{-s\iota} - \mu_1 s^{k_3} e^{-s\iota}, \quad \ell_{13} = 0, \quad \ell_{14} = 0,$
$\ell_{21} = 0, \quad \ell_{22} = s^{k_1} + h_2 s^{k_2} + q_2, \quad \ell_{23} = -\rho_2 e^{-s\iota} - \mu_2 s^{k_3} e^{-s\iota}, \quad \ell_{24} = 0,$
$\ell_{31} = 0, \quad \ell_{32} = 0, \quad \ell_{33} = s^{k_1} + h_3 s^{k_2} + q_3, \quad \ell_{34} = -\rho_3 e^{-s\iota} - \mu_3 s^{k_3} e^{-s\iota},$
$\ell_{41} = -\eta_1 e^{-s\iota} - \mu_4 s^{k_3} e^{-s\iota}, \quad \ell_{42} = -\eta_2 e^{-s\iota} - \mu_5 s^{k_3} e^{-s\iota}, \quad \ell_{43} = -\eta_3 e^{-s\iota} - \mu_6 s^{k_3} e^{-s\iota},$
$\ell_{44} = s^{k_1} + h_4 s^{k_2} + q_4.$

The above characteristic equation is equivalent to

$$\Phi_0(s) + \Phi_2(s)e^{-2s\iota} + \Phi_3(s)e^{-3s\iota} + \Phi_4(s)e^{-4s\iota} = 0, \tag{3}$$

where

$$\begin{aligned}
\Phi_0 = {} & q_1q_2q_3q_4 + (q_1q_2q_3 + q_1q_2q_4 + q_1q_3q_4 + q_2q_3q_4)s^{k_1} + (h_1q_2q_3q_4 + h_2q_1q_3q_4 \\
& + h_3q_1q_2q_4 + h_4q_1q_2q_3)s^{k_2} + (q_1q_2 + q_1q_3 + q_1q_4 + q_2q_3 + q_2q_4 + q_3q_4)s^{2k_1} \\
& + (h_1h_2q_3q_4 + h_1h_3q_2q_4 + h_1h_4q_2q_3 + h_2h_3q_1q_4 + h_2h_4q_1q_3 + h_3h_4q_1q_2)s^{2k_2} \\
& + (q_1 + q_2 + q_3 + q_4)s^{3k_1} + (h_1h_2h_3q_4 + h_1h_2h_4q_3 + h_1h_3h_4q_2 + h_2h_3h_4q_1)s^{3k_2} \\
& + s^{4k_1} + h_1h_2h_3h_4s^{4k_2} + (h_1q_2q_3 + h_1q_2q_4 + h_1q_3q_4 + h_2q_1q_3 + h_2q_1q_4 \\
& + h_2q_3q_4 + h_3q_1q_2 + h_3q_1q_4 + h_3q_2q_4 + h_4q_1q_2 + h_4q_1q_3 + h_4q_2q_3)s^{k_1+k_2} \\
& + (h_1h_2q_3 + h_1h_2q_4 + h_1h_3q_2 + h_1h_3q_4 + h_1h_4q_2 + h_1h_4q_3 + h_2h_3q_1 + h_2h_3q_4 \\
& + h_2h_4q_1 + h_2h_4q_3 + h_3h_4q_1 + h_3h_4q_2)s^{k_1+2k_2} + (h_1h_2h_3 + h_1h_2h_4 \\
& + h_1h_3h_4 + h_2h_3h_4)s^{k_1+3k_2} + (h_1q_2 + h_1q_3 + h_1q_4 + h_2q_1 + h_2q_3 + h_2q_4 \\
& + h_3q_1 + h_3q_2 + h_3q_4 + h_4q_1 + h_4q_2 + h_4q_3)s^{2k_1+k_2} + (h_1h_2 + h_1h_3 + h_1h_4 \\
& + h_2h_3 + h_2h_4 + h_3h_4)s^{2(k_1+k_2)} + (h_1 + h_2 + h_3 + h_4)s^{3k_1+k_2}, \\
\Phi_2 = {} & -\eta_3q_1q_2\rho_3 - \eta_3\rho_3s^{2k_1} - \eta_3h_1h_2\rho_3s^{2k_2} - \mu_3\mu_6q_1q_2s^{2k_3} - (\eta_3q_1\rho_3 \\
& + \eta_3q_2\rho_3)s^{k_1} - (\eta_3h_1q_2\rho_3 + \eta_3h_2q_1\rho_3)s^{k_2} - (\eta_3\mu_3q_1q_2 + \mu_6q_1q_2\rho_3)s^{k_3} \\
& - (\eta_3h_1\rho_3 + \eta_3h_2\rho_3)s^{k_1+k_2} - (\eta_3\mu_3q_1 + \eta_3\mu_3q_2 + \mu_6q_1\rho_3 + \mu_6q_2\rho_3)s^{k_1+k_3} \\
& - (\eta_3h_1\mu_3q_2 + \eta_3h_2\mu_3q_1 + h_1\mu_6q_2\rho_3 + h_2\mu_6q_1\rho_3)s^{k_2+k_3} - (\eta_3h_1\mu_3 + \eta_3h_2\mu_3 \\
& + h_1\mu_6\rho_3 + h_2\mu_6\rho_3)s^{k_1+k_2+k_3} - (\mu_3\mu_6q_1 + \mu_3\mu_6q_2)s^{k_1+2k_3} - (h_1\mu_3\mu_6q_2 \\
& + h_2\mu_3\mu_6q_1)s^{k_2+2k_3} - (\eta_3\mu_3 + \mu_6\rho_3)s^{2k_1+k_3} - (\eta_3h_1h_2\mu_3 + h_1h_2\mu_6\rho_3)s^{2k_2+k_3} \\
& - \mu_3\mu_6s^{2(k_1+k_3)} - h_1h_2\mu_3\mu_6s^{2(k_2+k_3)} - (h_1\mu_3\mu_6 + h_2\mu_3\mu_6)s^{k_1+k_2+2k_3}, \\
\Phi_3 = {} & -\eta_2q_1\rho_2\rho_3 - \eta_2\rho_2\rho_3s^{k_1} - \eta_2h_1\rho_2\rho_3s^{k_2} - (\eta_2\mu_2q_1\rho_3 + \eta_2\mu_3q_1\rho_2 + \mu_5q_1\rho_2\rho_3)s^{k_3} \\
& - (\eta_2\mu_2\mu_3q_1 + \mu_2\mu_5q_1\rho_3 + \mu_3\mu_5q_1\rho_2)s^{2k_3} - \mu_2\mu_3\mu_5q_1s^{3k_3} - (\eta_2\mu_2\rho_3 \\
& + \eta_2\mu_3\rho_2 + \mu_5\rho_2\rho_3)s^{k_1+k_3} - (\eta_2h_1\mu_2\rho_3 + \eta_2h_1\mu_3\rho_2 + h_1\mu_5\rho_2\rho_3)s^{k_2+k_3} \\
& - (\eta_2\mu_2\mu_3 + \mu_2\mu_5\rho_3 + \mu_3\mu_5\rho_2)s^{k_1+2k_3} - (\eta_2h_1\mu_2\mu_3 + h_1\mu_2\mu_5\rho_3 \\
& + h_1\mu_3\mu_5\rho_2)s^{k_2+2k_3} - \mu_2\mu_3\mu_5s^{k_1+3k_3} - h_1\mu_2\mu_3\mu_5s^{k_2+3k_3}, \\
\Phi_4 = {} & -\eta_1\rho_1\rho_2\rho_3 - (\eta_1\mu_1\rho_2\rho_3 + \eta_1\mu_2\rho_1\rho_3 + \eta_1\mu_3\rho_1\rho_2 + \mu_4\rho_1\rho_2\rho_3)s^{k_3} \\
& - (\eta_1\mu_1\mu_2\rho_3 + \eta_1\mu_1\mu_3\rho_2 + \eta_1\mu_2\mu_3\rho_1 + \mu_1\mu_4\rho_2\rho_3 + \mu_2\mu_4\rho_1\rho_3 \\
& + \mu_3\mu_4\rho_1\rho_2)s^{2k_3} - (\eta_1\mu_1\mu_2\mu_3 + \mu_1\mu_2\mu_4\rho_3 + \mu_1\mu_3\mu_4\rho_2 \\
& + \mu_2\mu_3\mu_4\rho_1)s^{3k_3} - \mu_1\mu_2\mu_3\mu_4s^{4k_3}.
\end{aligned}$$

If $\iota = 0$ in the characteristic Equation (3), then it follows that

$$\begin{aligned}
& \sigma_0 + \sigma_1s^{k_1} + \sigma_2s^{2k_1} + \sigma_3s^{3k_1} + \sigma_4s^{4k_1} + \sigma_5s^{k_2} + \sigma_6s^{2k_2} + \sigma_7s^{3k_2} + \sigma_8s^{4k_2} + \sigma_9s^{k_3} + \sigma_{10}s^{2k_3} \\
& + \sigma_{11}s^{3k_3} + \sigma_{12}s^{4k_3} + \sigma_{13}s^{k_1+k_2} + \sigma_{14}s^{k_1+k_3} + \sigma_{15}s^{k_2+k_3} + \sigma_{16}s^{k_1+k_2+k_3} + \sigma_{17}s^{k_1+2k_2} \\
& + \sigma_{18}s^{k_1+2k_3} + \sigma_{19}s^{k_2+2k_3} + \sigma_{20}s^{k_1+3k_2} + \sigma_{21}s^{k_1+3k_3} + \sigma_{22}s^{k_2+3k_3} + \sigma_{23}s^{2k_1+k_2} \\
& + \sigma_{24}s^{2k_1+k_3} + \sigma_{25}s^{2k_2+k_3} + \sigma_{26}s^{2k_1+2k_2} + \sigma_{27}s^{2k_1+2k_3} + \sigma_{28}s^{2k_2+2k_3} + \sigma_{29}s^{k_1+k_2+2k_3} = 0,
\end{aligned} \tag{4}$$

where

$$\begin{aligned}
\sigma_0 &= -\eta_1\rho_1\rho_2\rho_3 - \eta_2q_1\rho_2\rho_3 - \eta_3q_1q_2\rho_3 + q_1q_2q_3q_4, \\
\sigma_1 &= -(\eta_3q_2\rho_3 + q_1q_2q_3 + q_1q_2q_4 + q_1q_3q_4 + q_2q_3q_4 + \eta_2\rho_2\rho_3 + \eta_3q_1\rho_3), \\
\sigma_2 &= -(\eta_3\rho_3 - q_1q_2 - q_1q_3 - q_1q_4 - q_2q_3 - q_2q_4 - q_3q_4), \\
\sigma_3 &= q_1 + q_2 + q_3 + q_4, \\
\sigma_4 &= 1, \\
\sigma_5 &= -(\eta_2h_1\rho_2\rho_3 + \eta_3h_1q_2\rho_3 + \eta_3h_2q_1\rho_3 - h_1q_2q_3q_4 - h_2q_1q_3q_4 - h_3q_1q_2q_4 - h_4q_1q_2q_3),
\end{aligned}$$

$$
\begin{aligned}
\sigma_6 &= -(\eta_3 h_1 h_2 \rho_3 - h_1 h_2 q_3 q_4 - h_1 h_3 q_2 q_4 - h_1 h_4 q_2 q_3 - h_2 h_3 q_1 q_4 - h_2 h_4 q_1 q_3 - h_3 h_4 q_1 q_2),\\
\sigma_7 &= h_1 h_2 h_3 q_4 + h_1 h_2 h_4 q_3 + h_1 h_3 h_4 q_2 + h_2 h_3 h_4 q_1,\\
\sigma_8 &= h_1 h_2 h_3 h_4,\\
\sigma_9 &= -(\eta_1 \mu_1 \rho_2 \rho_3 + \eta_1 \mu_2 \rho_1 \rho_3 + \eta_1 \mu_3 \rho_1 \rho_2 + \mu_4 \rho_1 \rho_2 \rho_3 + \mu_5 q_1 \rho_2 \rho_3 + \mu_6 q_1 q_2 \rho_3 + \eta_2 \mu_2 q_1 \rho_3\\
&\quad + \eta_2 \mu_3 q_1 \rho_2 + \eta_3 \mu_3 q_1 q_2),\\
\sigma_{10} &= -(\eta_1 \mu_1 \mu_2 \rho_3 + \eta_1 \mu_1 \mu_3 \rho_2 + \eta_1 \mu_2 \mu_3 \rho_1 + \mu_1 \mu_4 \rho_2 \rho_3 + \mu_2 \mu_4 \rho_1 \rho_3 + \mu_3 \mu_6 q_1 q_2 + \eta_2 \mu_2 \mu_3 q_1\\
&\quad + \mu_2 \mu_5 q_1 \rho_3 + \mu_3 \mu_5 q_1 \rho_2 + \mu_3 \mu_4 \rho_1 \rho_2),\\
\sigma_{11} &= -(\eta_1 \mu_1 \mu_2 \mu_3 + \mu_1 \mu_2 \mu_4 \rho_3 + \mu_1 \mu_3 \mu_4 \rho_2 + \mu_2 \mu_3 \mu_4 \rho_1 + \mu_2 \mu_3 \mu_5 q_1),\\
\sigma_{12} &= -\mu_1 \mu_2 \mu_3 \mu_4,\\
\sigma_{13} &= -(\eta_3 h_1 \rho_3 + \eta_3 h_2 \rho_3 - h_1 q_2 q_3 - h_1 q_2 q_4 - h_1 q_3 q_4 - h_2 q_1 q_3 - h_2 q_1 q_4 - h_2 q_3 q_4 - h_3 q_1 q_2\\
&\quad - h_3 q_1 q_4 - h_3 q_2 q_4 - h_4 q_1 q_2 - h_4 q_1 q_3 - h_4 q_2 q_3),\\
\sigma_{14} &= -(\eta_2 \mu_2 \rho_3 + \eta_2 \mu_3 \rho_2 + \eta_3 \mu_3 q_1 + \eta_3 \mu_3 q_2 + \mu_5 \rho_2 \rho_3 + \mu_6 q_1 \rho_3 + \mu_6 q_2 \rho_3),\\
\sigma_{15} &= -(\eta_2 h_1 \mu_2 \rho_3 + \eta_2 h_1 \mu_3 \rho_2 + \eta_3 h_1 \mu_3 q_2 + \eta_3 h_2 \mu_3 q_1 + h_1 \mu_5 \rho_2 \rho_3 + h_1 \mu_6 q_2 \rho_3 + h_2 \mu_6 q_1 \rho_3),\\
\sigma_{16} &= -(\eta_3 h_1 \mu_3 + \eta_3 h_2 \mu_3 + h_1 \mu_6 \rho_3 + h_2 \mu_6 \rho_3),\\
\sigma_{17} &= h_1 h_2 q_3 + h_1 h_2 q_4 + h_1 h_3 q_2 + h_1 h_3 q_4 + h_1 h_4 q_2 + h_1 h_4 q_3 + h_2 h_3 q_1 + h_2 h_3 q_4 + h_2 h_4 q_1\\
&\quad + h_2 h_4 q_3 + h_3 h_4 q_1 + h_3 h_4 q_2,\\
\sigma_{18} &= -(\eta_2 \mu_2 \mu_3 + \mu_2 \mu_5 \rho_3 + \mu_3 \mu_5 \rho_2 + \mu_3 \mu_6 q_1 + \mu_3 \mu_6 q_2),\\
\sigma_{19} &= -(\eta_2 h_1 \mu_2 \mu_3 + h_1 \mu_2 \mu_5 \rho_3 + h_1 \mu_3 \mu_5 \rho_2 + h_1 \mu_3 \mu_6 q_2 + h_2 \mu_3 \mu_6 q_1),\\
\sigma_{20} &= h_1 h_2 h_3 + h_1 h_2 h_4 + h_1 h_3 h_4 + h_2 h_3 h_4,\\
\sigma_{21} &= -\mu_2 \mu_3 \mu_5,\\
\sigma_{22} &= -h_1 \mu_2 \mu_3 \mu_5,\\
\sigma_{23} &= h_1 q_2 + h_1 q_3 + h_1 q_4 + h_2 q_1 + h_2 q_3 + h_2 q_4 + h_3 q_1 + h_3 q_2 + h_3 q_4 + h_4 q_1 + h_4 q_2 + h_4 q_3,\\
\sigma_{24} &= -(\mu_6 \rho_3 + \eta_3 \mu_3),\\
\sigma_{25} &= -(\eta_3 h_1 h_2 \mu_3 + h_1 h_2 \mu_6 \rho_3),\\
\sigma_{26} &= h_1 h_3 + h_1 h_4 + h_2 h_3 + h_2 h_4 + h_3 h_4 + h_1 h_2,\\
\sigma_{27} &= -\mu_3 \mu_6,\\
\sigma_{28} &= -h_1 h_2 \mu_3 \mu_6,\\
\sigma_{29} &= -(h_1 \mu_3 \mu_6 + h_2 \mu_3 \mu_6).
\end{aligned}
$$

By employing corollary from [35], we derive that all roots of Equation (4) have negative real parts. Therefore, we directly determine that system (1) is asymptotically stable when $\iota = 0$.

By multiplying Equation (3) by $e^{s\iota}$, $e^{2s\iota}$ and $e^{3s\iota}$, respectively. Then we conclude that

$$
\begin{cases}
\Phi_0(s)e^{s\iota} + \Phi_2(s)e^{-s\iota} + \Phi_3(s)e^{-2s\iota} + \Phi_4(s)e^{-3s\iota} = 0,\\
\Phi_0(s)e^{2s\iota} + \Phi_2(s) + \Phi_3(s)e^{-s\iota} + \Phi_4(s)e^{-2s\iota} = 0,\\
\Phi_0(s)e^{3s\iota} + \Phi_2(s)e^{s\iota} + \Phi_3(s) + \Phi_4(s)e^{-s\iota} = 0.
\end{cases} \tag{5}
$$

To facilitate the following deduction, we mark the real part and imaginary part of $\Phi_\kappa(s)(\kappa = 0, 1, 2)$ as Φ_κ^R, Φ_κ^I, respectively. Let $s = w(\cos\frac{\pi}{2} + i\sin\frac{\pi}{2})(w > 0)$ be a pure imaginary root of Equation (5). Then the following equations are obtained.

$$
\begin{cases}
\xi_{11}\cos w\iota+\xi_{12}\sin w\iota+\xi_{13}\cos 2w\iota+\xi_{14}\sin 2w\iota+\xi_{15}\cos 3w\iota+\xi_{16}\sin 3w\iota=\xi_{17},\\
\xi_{21}\cos w\iota+\xi_{22}\sin w\iota+\xi_{23}\cos 2w\iota+\xi_{24}\sin 2w\iota+\xi_{25}\cos 3w\iota+\xi_{26}\sin 3w\iota=\xi_{27},\\
\xi_{31}\cos w\iota+\xi_{32}\sin w\iota+\xi_{33}\cos 2w\iota+\xi_{34}\sin 2w\iota+\xi_{35}\cos 3w\iota+\xi_{36}\sin 3w\iota=\xi_{37},\\
\xi_{41}\cos w\iota+\xi_{42}\sin w\iota+\xi_{43}\cos 2w\iota+\xi_{44}\sin 2w\iota+\xi_{45}\cos 3w\iota+\xi_{46}\sin 3w\iota=\xi_{47},\\
\xi_{51}\cos w\iota+\xi_{52}\sin w\iota+\xi_{53}\cos 2w\iota+\xi_{54}\sin 2w\iota+\xi_{55}\cos 3w\iota+\xi_{56}\sin 3w\iota=\xi_{57},\\
\xi_{61}\cos w\iota+\xi_{62}\sin w\iota+\xi_{63}\cos 2w\iota+\xi_{64}\sin 2w\iota+\xi_{65}\cos 3w\iota+\xi_{66}\sin 3w\iota=\xi_{67},
\end{cases}
\tag{6}
$$

where

$\xi_{11}=\Phi_0^R+\Phi_2^R,\quad \xi_{12}=\Phi_2^I-\Phi_0^I,\quad \xi_{13}=\Phi_3^R,\quad \xi_{14}=\Phi_3^I,\quad \xi_{15}=\Phi_4^R,\quad \xi_{16}=\Phi_4^I,$
$\xi_{21}=\Phi_0^I+\Phi_2^I,\quad \xi_{22}=\Phi_0^R-\Phi_2^R,\quad \xi_{23}=\Phi_3^I,\quad \xi_{24}=-\Phi_3^R,\quad \xi_{25}=\Phi_4^I,\quad \xi_{26}=-\Phi_4^R,$
$\xi_{31}=\Phi_3^R,\quad \xi_{32}=\Phi_3^I,\quad \xi_{33}=\Phi_0^R+\Phi_4^R,\quad \xi_{34}=\Phi_4^I-\Phi_0^I,\quad \xi_{35}=0,\quad \xi_{36}=0,$
$\xi_{41}=\Phi_3^I,\quad \xi_{42}=-\Phi_3^R,\quad \xi_{43}=\Phi_0^I+\Phi_4^I,\quad \xi_{44}=\Phi_0^R-\Phi_4^R,\quad \xi_{45}=0,\quad \xi_{46}=0,$
$\xi_{51}=\Phi_2^R+\Phi_4^R,\quad \xi_{52}=\Phi_4^I-\Phi_2^I,\quad \xi_{53}=0,\quad \xi_{54}=0,\quad \xi_{55}=\Phi_0^R,\quad \xi_{56}=-\Phi_0^I,$
$\xi_{61}=\Phi_2^I+\Phi_4^I,\quad \xi_{62}=\Phi_2^R-\Phi_4^R,\quad \xi_{63}=0,\quad \xi_{64}=0,\quad \xi_{65}=\Phi_0^I,\quad \xi_{66}=\Phi_0^R,$
$\xi_{17}=0,\quad \xi_{27}=0,\quad \xi_{37}=-\Phi_2^R,\quad \xi_{47}=-\Phi_2^I,\quad \xi_{57}=-\Phi_3^R,\quad \xi_{67}=-\Phi_3^I.$

Accordingly, the determinant for the coefficient matrix of Equation (6) can be obtained as

$$
\Theta_1=\begin{vmatrix}
\xi_{11}&\xi_{12}&\xi_{13}&\xi_{14}&\xi_{15}&\xi_{16}\\
\xi_{21}&\xi_{22}&\xi_{23}&\xi_{24}&\xi_{25}&\xi_{26}\\
\xi_{31}&\xi_{32}&\xi_{33}&\xi_{34}&\xi_{35}&\xi_{36}\\
\xi_{41}&\xi_{42}&\xi_{43}&\xi_{44}&\xi_{45}&\xi_{46}\\
\xi_{51}&\xi_{52}&\xi_{53}&\xi_{54}&\xi_{55}&\xi_{56}\\
\xi_{61}&\xi_{62}&\xi_{63}&\xi_{64}&\xi_{65}&\xi_{66}
\end{vmatrix}.
$$

By using Cramer's rule and Equation (6), we promptly obtain the following equations:

$$
\begin{cases}
\cos 2w\iota=\dfrac{\Theta_2}{\Theta_1}=\nabla_1(w),\\
\sin 2w\iota=\dfrac{\Theta_3}{\Theta_1}=\nabla_2(w),
\end{cases}
\tag{7}
$$

where

$$
\Theta_2=\begin{vmatrix}
\xi_{17}&\xi_{12}&\xi_{13}&\xi_{14}&\xi_{15}&\xi_{16}\\
\xi_{27}&\xi_{22}&\xi_{23}&\xi_{24}&\xi_{25}&\xi_{26}\\
\xi_{37}&\xi_{32}&\xi_{33}&\xi_{34}&\xi_{35}&\xi_{36}\\
\xi_{47}&\xi_{42}&\xi_{43}&\xi_{44}&\xi_{45}&\xi_{46}\\
\xi_{57}&\xi_{52}&\xi_{53}&\xi_{54}&\xi_{55}&\xi_{56}\\
\xi_{67}&\xi_{62}&\xi_{63}&\xi_{64}&\xi_{65}&\xi_{66}
\end{vmatrix},
$$

$$
\Theta_3=\begin{vmatrix}
\xi_{11}&\xi_{17}&\xi_{13}&\xi_{14}&\xi_{15}&\xi_{16}\\
\xi_{21}&\xi_{27}&\xi_{23}&\xi_{24}&\xi_{25}&\xi_{26}\\
\xi_{31}&\xi_{37}&\xi_{33}&\xi_{34}&\xi_{35}&\xi_{36}\\
\xi_{41}&\xi_{47}&\xi_{43}&\xi_{44}&\xi_{45}&\xi_{46}\\
\xi_{51}&\xi_{57}&\xi_{53}&\xi_{54}&\xi_{55}&\xi_{56}\\
\xi_{61}&\xi_{67}&\xi_{63}&\xi_{64}&\xi_{65}&\xi_{66}
\end{vmatrix}.
$$

It can be derived from Equation (7) that

$$
\nabla_1^2(w)+\nabla_2^2(w)=1, \tag{8}
$$

$$
\cos 2w\iota=\nabla_1(w). \tag{9}
$$

To acquire the main results, we propose the following assumption:

Hypothesis 2 (H2). *Equation (8) has at least a positive real root.*

According to Equation (9), we can clearly observe that expression of $\iota_1^{(\kappa)}$ as

$$\iota_1^{(\kappa)} = \frac{1}{2w}\Big[\arccos\nabla_1(w) + 2k\pi\Big], \quad \kappa = 0, 1, 2, \dots. \tag{10}$$

Therefore, the bifurcation points can be quickly deduced

$$\iota_0 = \min\{\iota_1^{(\kappa)}\}, \quad \kappa = 0, 1, 2, \dots, \tag{11}$$

where $\iota_1^{(\kappa)}$ is defined by Equation (10).

Remark 3. *For the derivation of bifurcation critical values, we can adopt traditional derivation methods, that is the direct method to solve the eigenvalues. However, in this article, we use the analytical method of characteristic equations and Cramer's rule to complete the derivation.*

The following assumption is essential for more precise bifurcation conditions.

Hypothesis 3 (H3). $\frac{\vartheta_1\varrho_1+\vartheta_2\varrho_2}{\varrho_1^2+\varrho_2^2} > 0$*, where* ϑ_1*,*ϑ_2*,* ϱ_1*,*ϱ_2 *are characterized in Equation (14).*

Lemma 1. *Let* $s(\iota) = \delta(\iota) + iw(\iota)$ *be the root of Equation (3) near* $\iota = \iota_0$ *conforming to* $\delta(\iota_0) = 0$*,* $w(\iota_0) = w_0$*. Based on this, the following horizontal condition hold true*

$$\mathrm{Re}\Big[\frac{ds}{d\iota}\Big]\Big|_{(\iota=\iota_0, w=w_0)} > 0.$$

Proof. Using the implicit function theorem to distinguish ι in Equation (3), we confirm

$$\begin{aligned}
&\Phi_0'(s)\frac{ds}{d\iota} + \Big[\Phi_2'(s)\frac{ds}{d\iota}e^{-2s\iota} + \Phi_2(s)e^{-2s\iota}\Big(-2\iota\frac{ds}{d\iota} - 2s\Big)\Big] \\
&+ \Big[\Phi_3'(s)\frac{ds}{d\iota}e^{-3s\iota} + \Phi_3(s)e^{-3s\iota}\Big(-3\iota\frac{ds}{d\iota} - 3s\Big)\Big] \\
&+ \Big[\Phi_4'(s)\frac{ds}{d\iota}e^{-4s\iota} + \Phi_4(s)e^{-4s\iota}\Big(-4\iota\frac{ds}{d\iota} - 4s\Big)\Big] = 0.
\end{aligned} \tag{12}$$

Through Equation (12) , we can gain that

$$\frac{ds}{d\iota} = \frac{\vartheta(s)}{\varrho(s)}, \tag{13}$$

where

$$\begin{aligned}
\vartheta(s) &= s[2\Phi_2(s)e^{-2s\iota} + 3\Phi_3(s)e^{-3s\iota} + 4\Phi_4(s)e^{-4s\iota}], \\
\varrho(s) &= \Phi_0'(s) + [\Phi_2'(s) - 2\iota\Phi_2(s)]e^{-2s\iota} + [\Phi_3'(s) - 3\iota\Phi_3(s)]e^{-3s\iota} \\
&\quad + [\Phi_4'(s) - 4\iota\Phi_4(s)]e^{-4s\iota}.
\end{aligned}$$

With the support of Equation (13) , it can be concluded that

$$\mathrm{Re}\Big[\frac{ds}{d\iota}\Big]\Big|_{(\iota=\iota_0, w=w_0)} = \frac{\vartheta_1\varrho_1 + \vartheta_2\varrho_2}{\varrho_1^2 + \varrho_2^2}, \tag{14}$$

where

$$
\begin{aligned}
\vartheta_1 &= w_0(2\Phi_2^R \sin 2w_0\iota_0 - 2\Phi_2^I \cos 2w_0\iota_0 + 3\Phi_3^R \sin 3w_0\iota_0 - 3\Phi_3^I \cos 3w_0\iota_0 \\
&\quad + 4\Phi_4^R \sin 4w_0\iota_0 - 4\Phi_4^I \cos 4w_0\iota_0), \\
\vartheta_2 &= w_0(2\Phi_1^R \cos 2w_0\iota_0 + 2\Phi_1^I \sin 2w_0\iota_0 + 4\Phi_2^R \cos 3w_0\iota_0 + 3\Phi_3^I \sin 3w_0\iota_0 \\
&\quad + 4\Phi_4^R \cos 4w_0\iota_0 + 4\Phi_4^I \sin 4w_0\iota_0), \\
\varrho_1 &= \Phi_0^{'R} + (\Phi_2^{'R} - 2\iota_0\Phi_2^R) \cos 2w_0\iota_0 + (\Phi_2^{'I} - 2\iota_0\Phi_2^I) \sin 2w_0\iota_0 \\
&\quad + (\Phi_3^{'R} - 3\iota_0\Phi_3^R) \cos 3w_0\iota_0 + (\Phi_3^{'I} - 3\iota_0\Phi_3^I) \sin 3w_0\iota_0 \\
&\quad + (\Phi_4^{'R} - 4\iota_0\Phi_4^R) \cos 4w_0\iota_0 + (\Phi_4^{'I} - 4\iota_0\Phi_4^I) \sin 4w_0\iota_0, \\
\varrho_2 &= \Phi_0^{'I} + (\Phi_2^{'I} - 2\iota_0\Re_2^I) \cos 2w_0\iota_0 - (\Phi_2^{'R} - 2\iota_0\Phi_2^R) \sin 2w_0\iota_0 \\
&\quad + (\Phi_3^{'I} - 3\iota_0\Phi_3^I) \cos 3w_0\iota_0 - (\Phi_3^{'R} - 3\iota_0\Phi_3^R) \sin 3w_0\iota_0 \\
&\quad + (\Phi_4^{'I} - 4\iota_0\Phi_4^I) \cos 4w_0\iota_0 - (\Phi_4^{'R} - 4\iota_0\Phi_4^R) \sin 4w_0\iota_0.
\end{aligned}
$$

Under the condition of satisfying the Hypothesis 3, the proof of Lemma 1 is achieved. □

The above has laid a solid foundation for proving the correctness of the following theorem.

Theorem 1. *By establishing assumptions Hypothesis 1–3, the following key achievements are observed.*

(1) *If $\iota \in [0, \iota_0)$, system (1) can displays the asymptotical steadiness of its equilibrium origin point.*
(2) *When $\iota = \iota_0$, system (1) undergoes a Hopf bifurcation at the origin.*

Remark 4. *For the analysis of case $\iota \neq 0$, in Section 5, we determine the bifurcation critical values based on the Equation (11) . This verifies the establishment of the lateral condition for Theorem 1.*

Remark 5. *In order to visually observe the stability of the system based on bifurcation critical values, we draw trajectories and phase graphs in both numerical simulations. When delay parameters are less than critical values, systems are stable, but when parameters are greater than critical values, systems bifurcate. Moreover, we also find that besides time delay, the variation of fractional orders also has effect on system stability. In Figure 1 in Example 1 and Figure 2 in Example 2, we depict the change of critical bifurcation value of the system with only a fractional order is altered.*

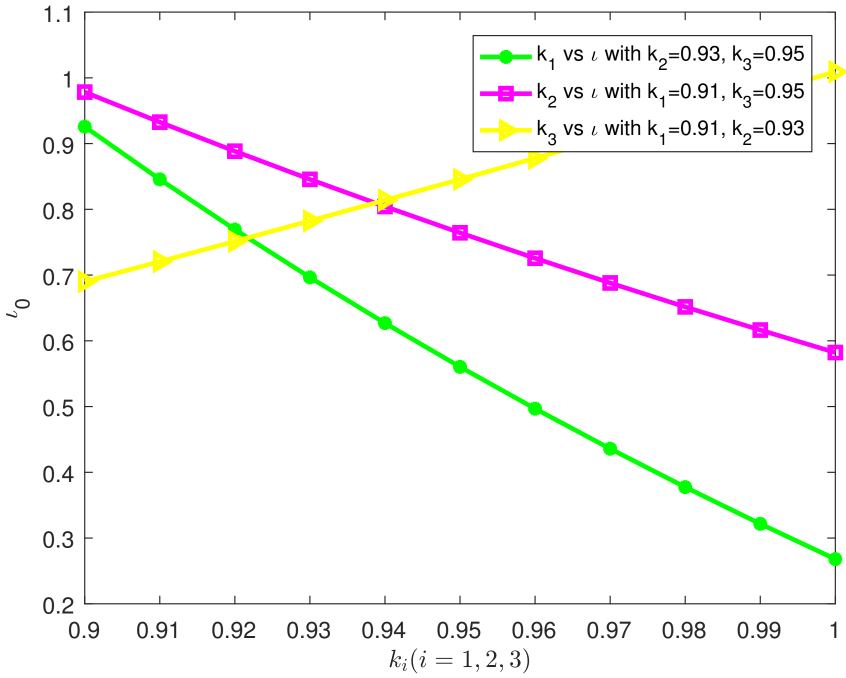

Figure 1. Bifurcation point ι_0 of FONTINN (15) depending on fractional orders.

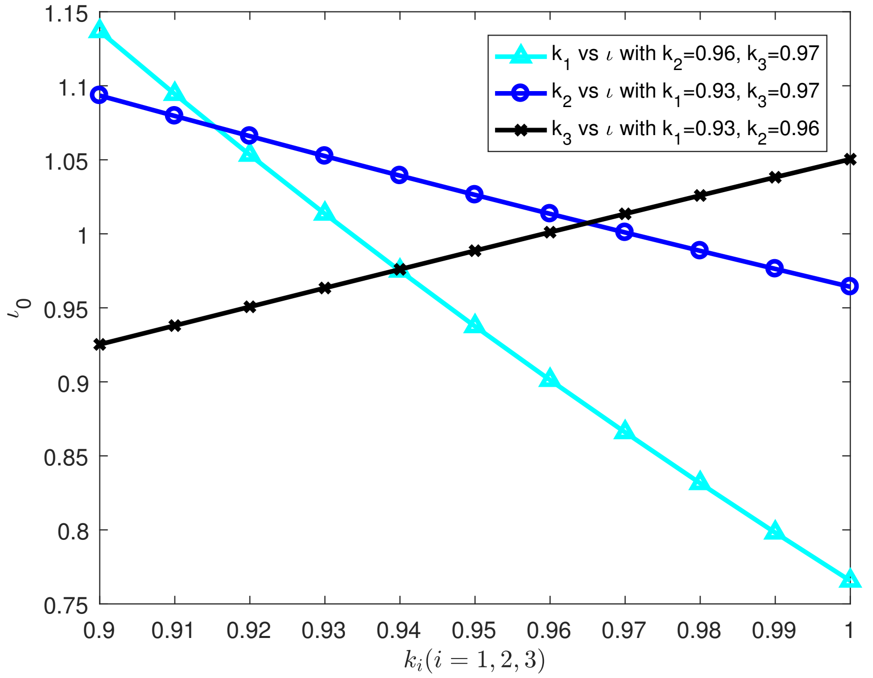

Figure 2. Bifurcation point ι_0 of FONTINN (16) depending on fractional orders.

Remark 6. *To make the research more valuable, we compare the bifurcation critical values of integer-order systems and fractional-order systems. By calculating and drawing Figures 3–6 in Example 1 and Figures 7–10 in Example 2, it can be concluded that fractional-order systems have better stability.*

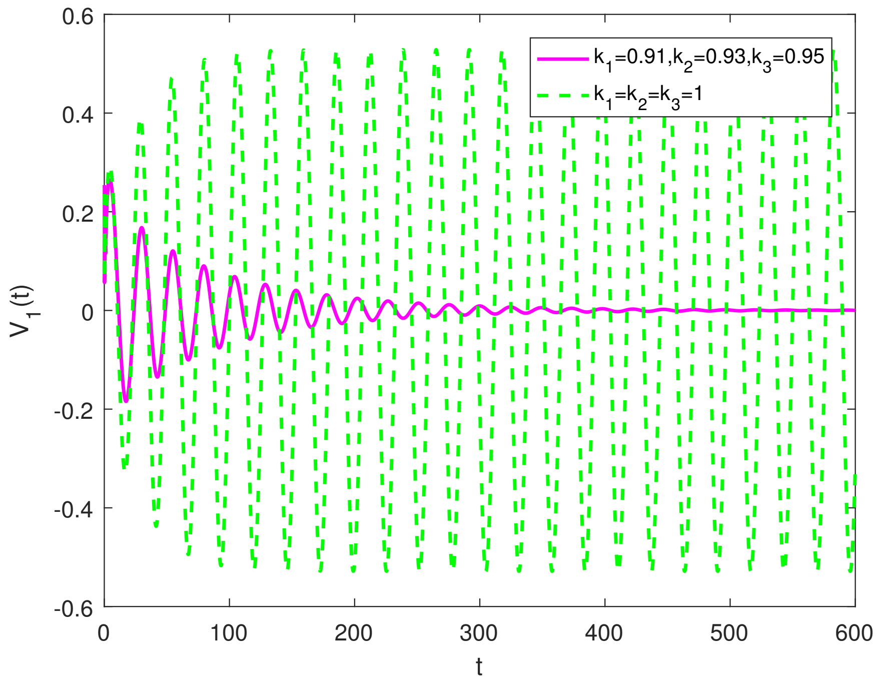

Figure 3. Comparisons on stability of FONTINN (15) between fractional-order case and integer-order case.

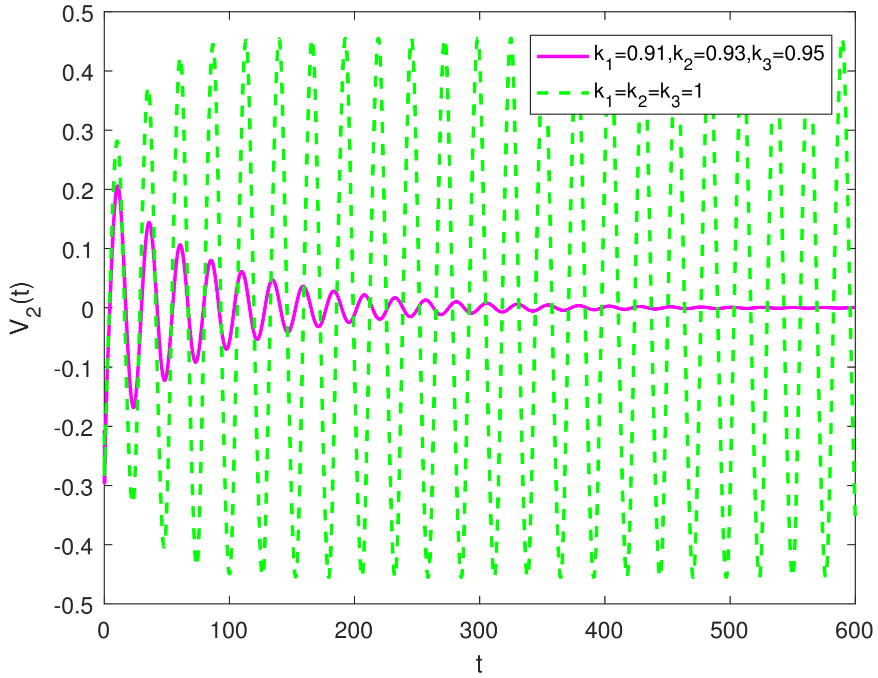

Figure 4. Comparisons on stability of FONTINN (15) between fractional-order case and integer-order case.

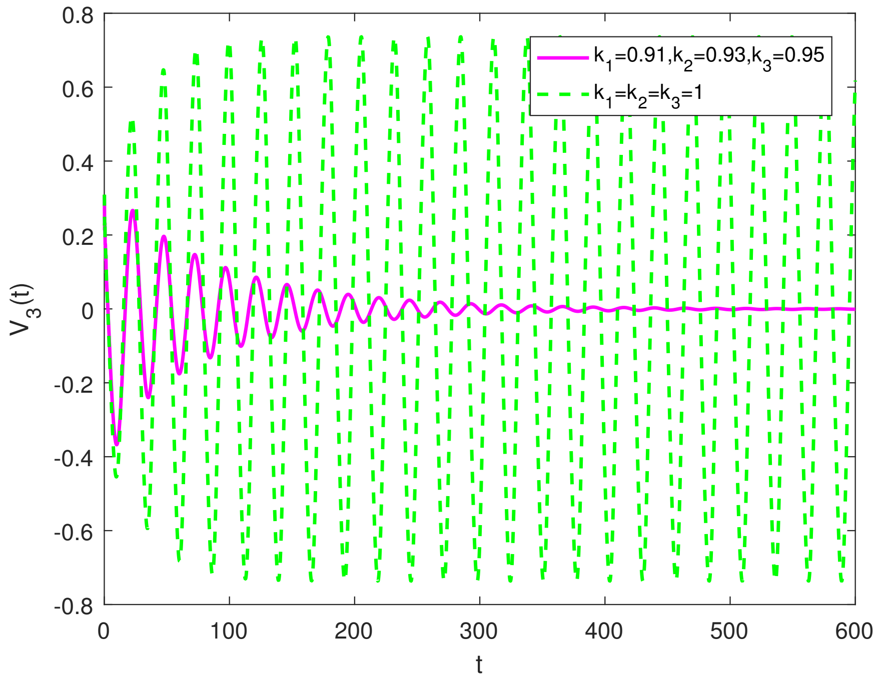

Figure 5. Comparisons on stability of FONTINN (15) between fractional-order case and integer-order case.

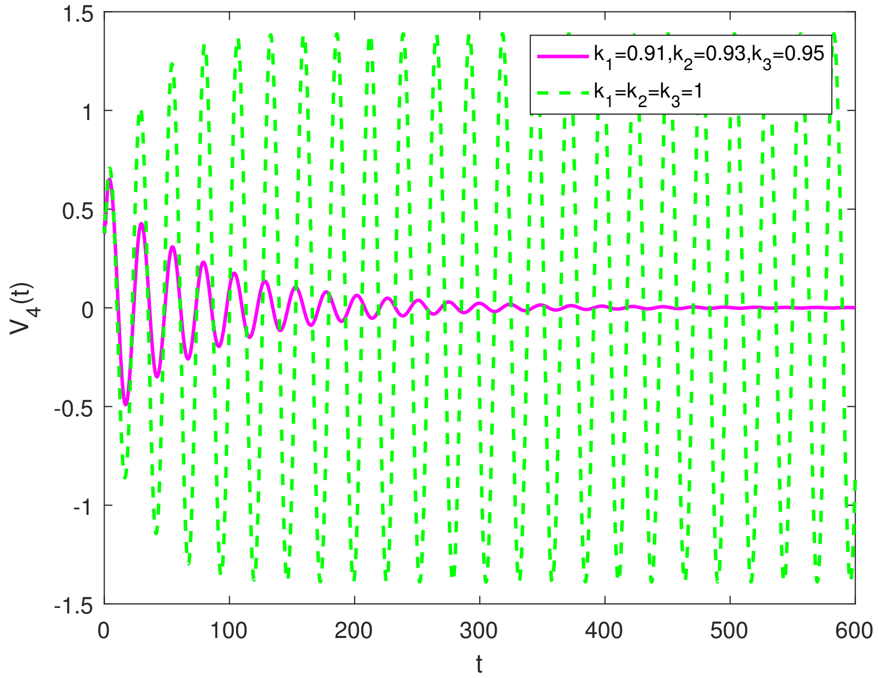

Figure 6. Comparisons on stability of FONTINN (15) between fractional-order case and integer-order case.

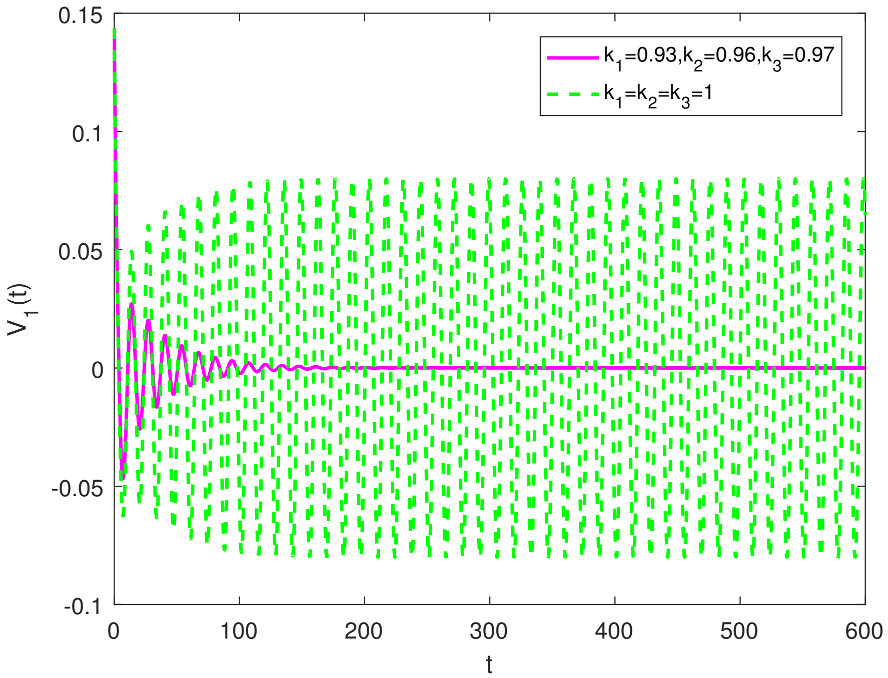

Figure 7. Comparisons on stability of FONTINN (16) between fractional-order case and integer-order case.

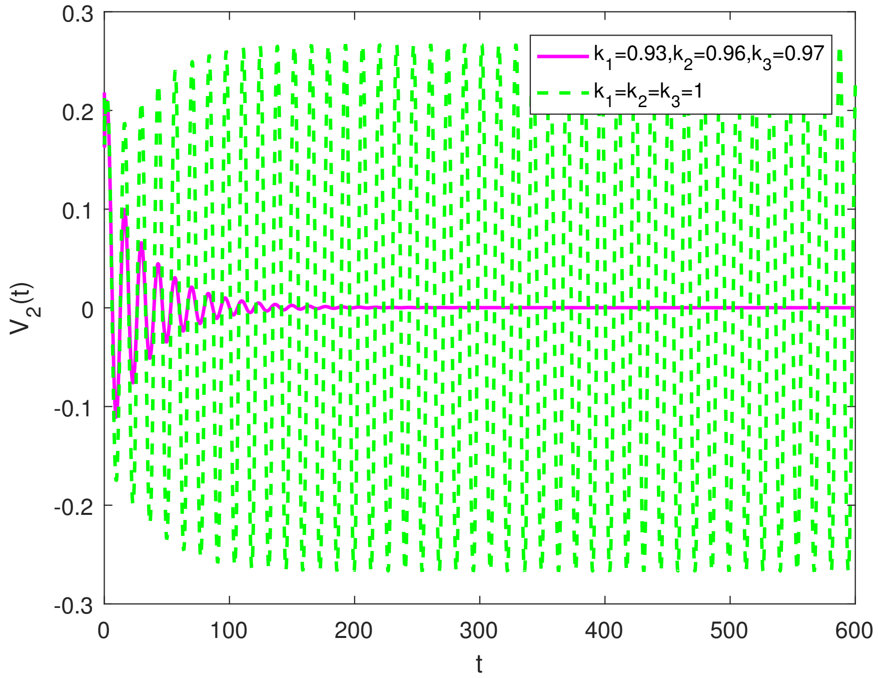

Figure 8. Comparisons on stability of FONTINN (16) between fractional-order case and integer-order case.

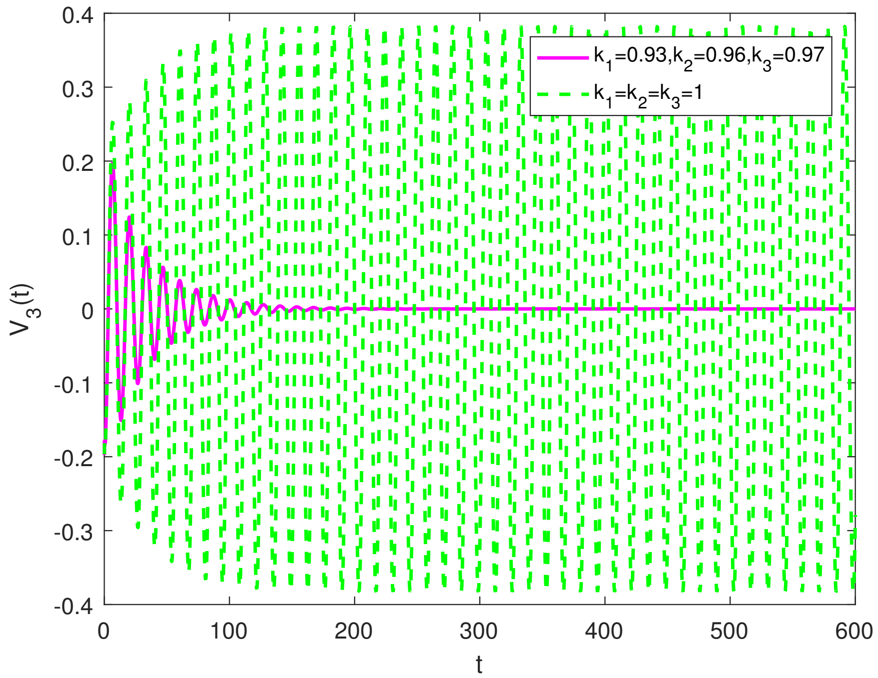

Figure 9. Comparisons on stability of FONTINN (16) between fractional-order case and integer-order case.

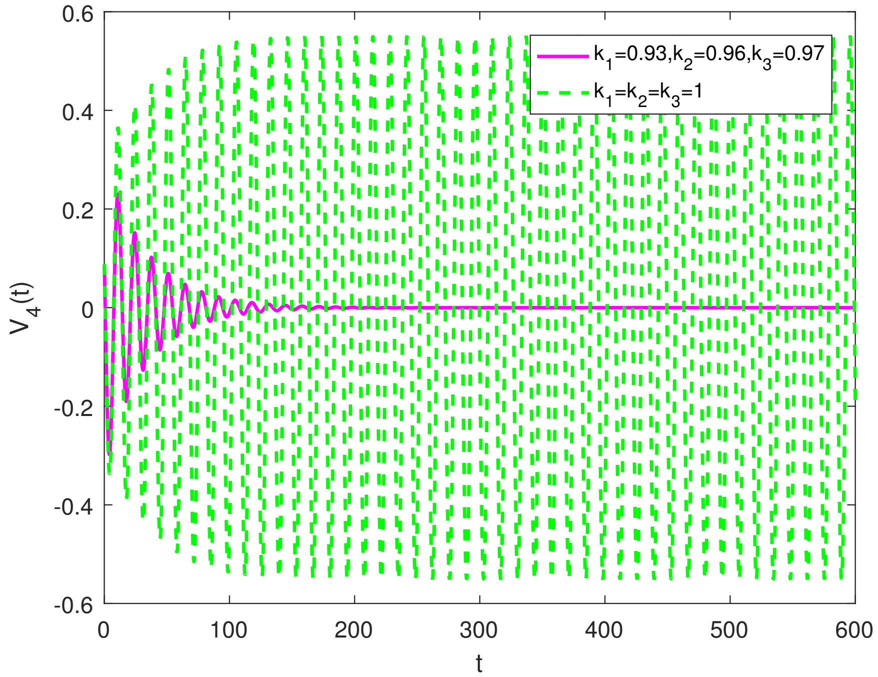

Figure 10. Comparisons on stability of FONTINN (16) between fractional-order case and integer-order case.

5. Experimental Verifications

To prove the correctness of the obtained theory, we conduct two numerical simulation experiments in this section.

5.1. Example 1

To start with, the first example to be considered as

$$\begin{cases} D^{k_1}V_1(t) = -0.6D^{k_2}V_1(t) - 0.2V_1(t) - 0.5F(V_2(t-\iota)) + 0.8D^{k_3}V_2(t-\iota), \\ D^{k_1}V_2(t) = -0.4D^{k_2}V_2(t) - 0.3V_2(t) - 0.2F(V_3(t-\iota)) - 0.9D^{k_3}V_3(t-\iota), \\ D^{k_1}V_3(t) = -0.8D^{k_2}V_3(t) - 0.4V_3(t) - 0.4F(V_4(t-\iota)) + 0.5D^{k_3}V_4(t-\iota), \\ D^{k_1}V_4(t) = -0.5D^{k_2}V_4(t) - 0.2V_4(t) + 0.5G(V_1(t-\iota)) - 0.5G(V_2(t-\iota)) + 0.4G(V_3(t-\iota)) \\ \qquad\qquad + 0.6D^{k_3}V_1(t-\iota) + 0.6D^{k_3}V_2(t-\iota) + 0.3D^{k_3}V_3(t-\iota). \end{cases} \tag{15}$$

We stipulate the activation function as $F(\cdot) = G(\cdot) = \tanh(\cdot)$, the initial value as $(V_1(0), V_2(0), V_3(0), V_4(0)) = (0.2, -0.2, 0.3, 0.4)$, and the fractional orders as $k_1 = 0.91, k_2 = 0.93, k_3 = 0.95$. Using Equation (11), we can accurately calculate that $w_0 = 0.2474, \iota_0 = 0.8456$. The assumption $\mathrm{Re}\left[\frac{ds}{d\iota}\right]\Big|_{(\iota=\iota_0, w=w_0)} = 0.2184 > 0$, which is verified in Hypothesis 3. The asymptotic stability of the zero equilibrium point of FONTINN (15) when $\iota = 0.65 < \iota_0 = 0.8456$ is depicted in Figures 11 and 12. In addition, the volatility of the zero equilibrium point of FONTINN (15) is illustrated and Hopf bifurcation occur when $\iota = 0.95 > \iota_0 = 0.8456$ are displayed in Figures 13 and 14.

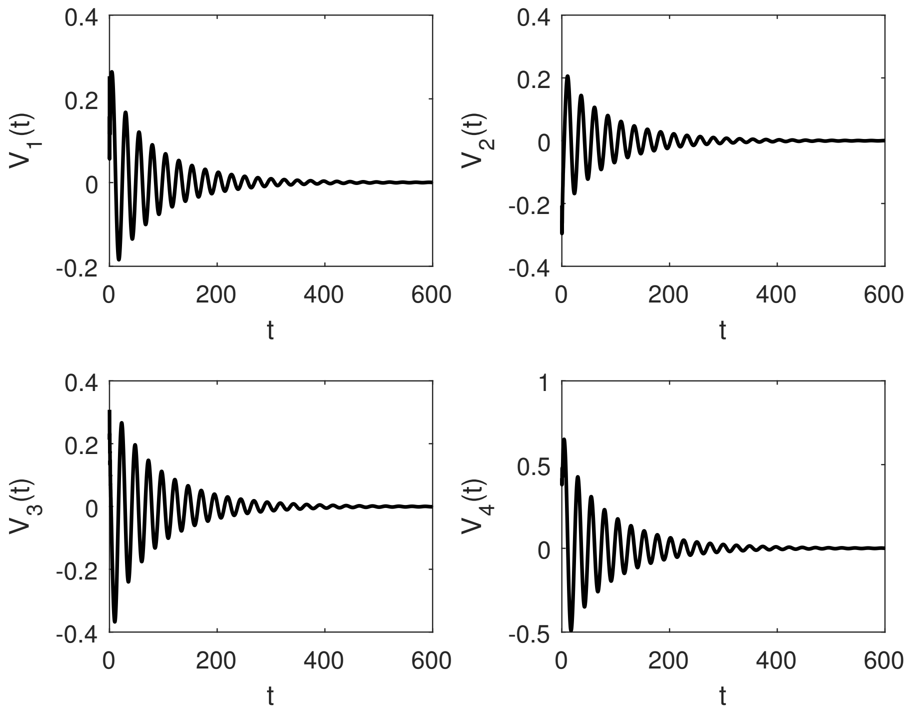

Figure 11. Trajectories of FONTINN (15) with $\iota = 0.65 < \iota_0 = 0.8456$.

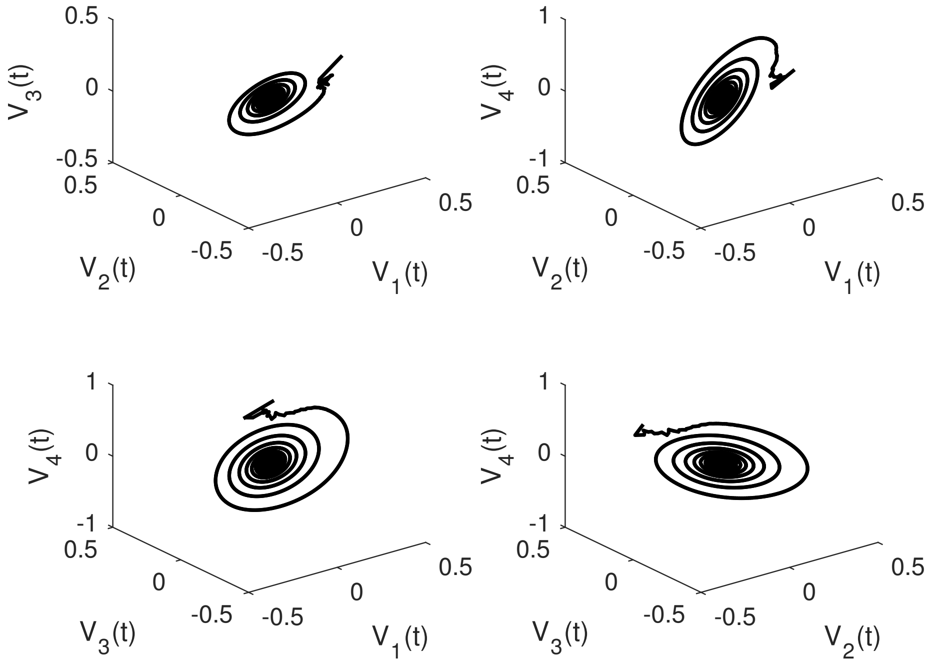

Figure 12. The portraits of FONTINN (15) with $\iota = 0.65 < \iota_0 = 0.8456$.

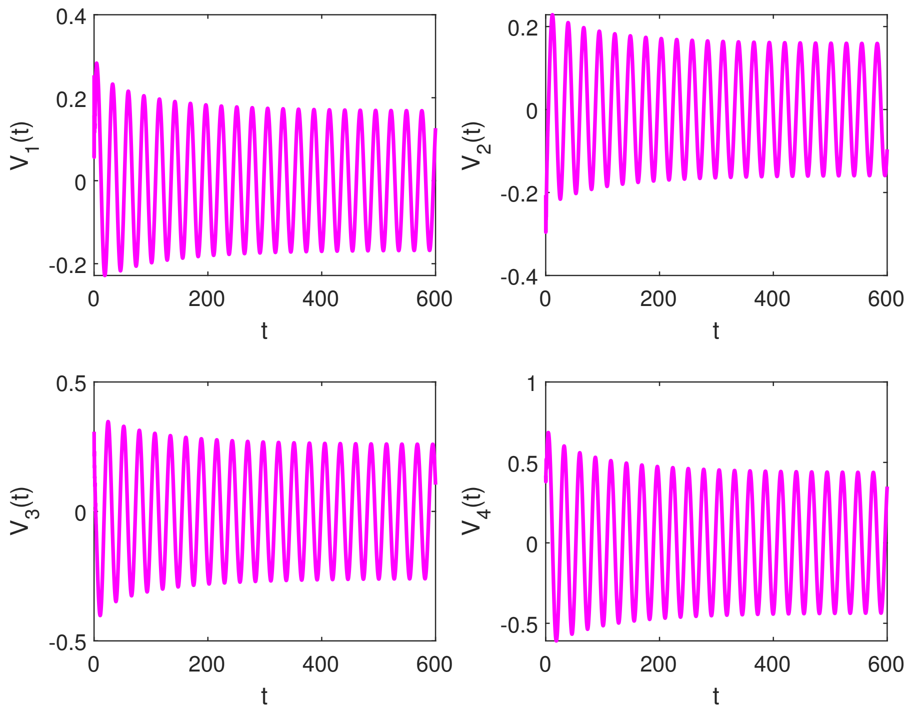

Figure 13. Trajectories of FONTINN ([15](#)) with $\iota = 0.95 > \iota_0 = 0.8456$.

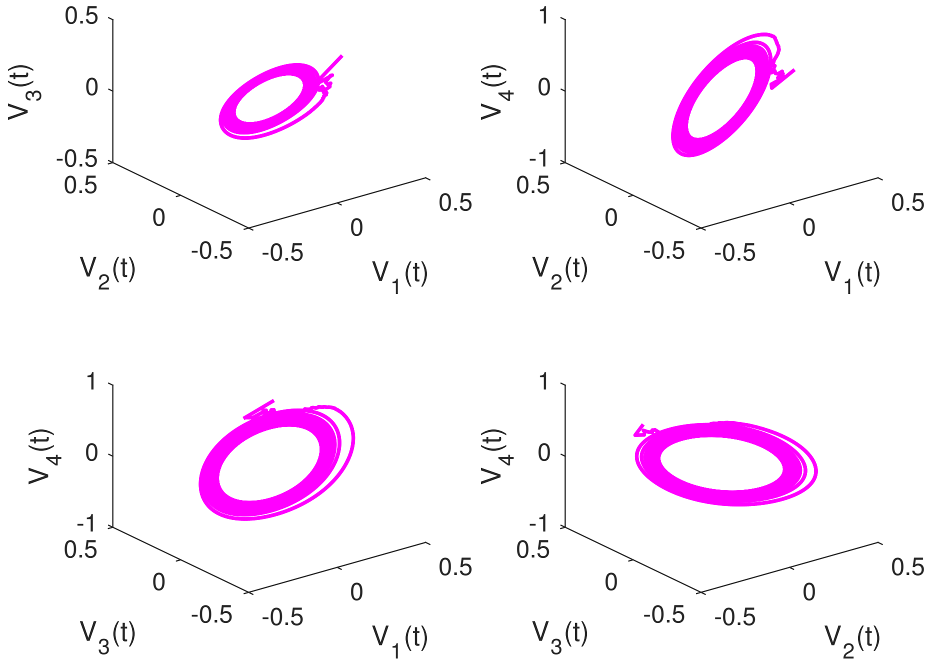

Figure 14. The portraits of FONTINN (15) with $\iota = 0.95 > \iota_0 = 0.8456$.

The critical bifurcation value of the system will change. By calculating, we obtain that $\tilde{w}_0 = 0.3237$, $\tilde{\iota}_0 = 0.1829 < \iota_0 = 0.8456$. It is obvious that the bifurcation critical value of integer order system is smaller than the value of fractional-order system. The difference with regard to stability between integer-order system and fractional-order system can be more clearly observed in Figures 3–6. According to this discovery, fractional-order neural networks have better ability to improve system stability compared with integer-order neural networks. It can be noticed from Figure 1 that the impact of fractional order on system stability is illustrated.

5.2. Example 2

Subsequently, the second example to be considered as

$$\begin{cases} D^{k_1}V_1(t) = -0.4D^{k_2}V_1(t) - 0.3V_1(t) - 0.2F(V_2(t-\iota)) + 0.2D^{k_3}V_2(t-\iota), \\ D^{k_1}V_2(t) = -0.6D^{k_2}V_2(t) - 0.4V_2(t) - 0.6F(V_3(t-\iota)) - 0.2D^{k_3}V_3(t-\iota), \\ D^{k_1}V_3(t) = -0.4D^{k_2}V_3(t) - 0.3V_3(t) - 0.5F(V_4(t-\iota)) - 0.4D^{k_3}V_4(t-\iota), \\ D^{k_1}V_4(t) = -0.2D^{k_2}V_4(t) - 0.3V_4(t) + 0.3G(V_1(t-\iota)) - 0.4G(V_2(t-\iota)) + 0.6G(V_3(t-\iota)) \\ \qquad\qquad + 0.6D^{k_3}V_1(t-\iota) - 0.7D^{k_3}V_2(t-\iota) - 0.4D^{k_3}V_3(t-\iota). \end{cases} \tag{16}$$

We stipulate the activation function as $F(\cdot) = G(\cdot) = \tanh(\cdot)$, the initial value as $(V_1(0), V_2(0), V_3(0), V_4(0)) = (0.15, 0.2, -0.2, 0.1)$, and the fractional orders as $k_1 = 0.93, k_2 = 0.96, k_3 = 0.97$. Using Equation (11), we can accurately calculate that $w_0 = 0.4486, \iota_0 = 1.0135$. We compute that the assumption $\mathrm{Re}\left[\frac{ds}{d\iota}\right]\Big|_{(\iota=\iota_0, w=w_0)} = 0.3512 > 0$, which satisfies Hypothesis 3. Based on Figures 15 and 16, the asymptotic stability of the zero equilibrium point of FONTINN (16) when $\iota = 0.85 < \iota_0 = 1.0135$ is presented. The volatility of the zero equilibrium point of FONTINN (16) and Hopf bifurcation begins to occur when $\iota = 1.1 > \iota_0 = 1.0135$ are shown in Figures 17 and 18.

By calculating, we obtain that $\tilde{w}_0 = 0.4984, \tilde{\iota}_0 = 0.7537 < \iota_0 = 1.0135$. It is obvious that the bifurcation critical value of integer-order system is smaller than the value of fractional order system. The difference with regard to stability between integer-order system and fractional-order system can be more clearly observed in Figures 7–10. According to this discovery, fractional-order neural networks have better ability to improve system stability compared to integer-order neural networks. It can be directly spotted from Figure 2 that impact of fractional order on system stability is evident.

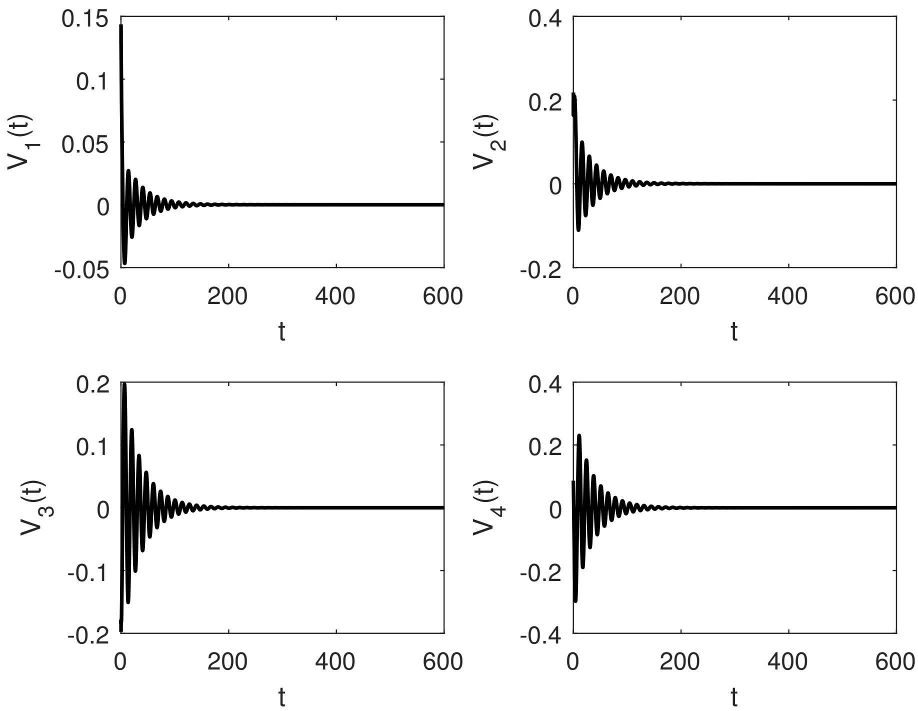

Figure 15. Trajectories of FONTINN (16) with $\iota = 0.85 < \iota_0 = 1.0135$.

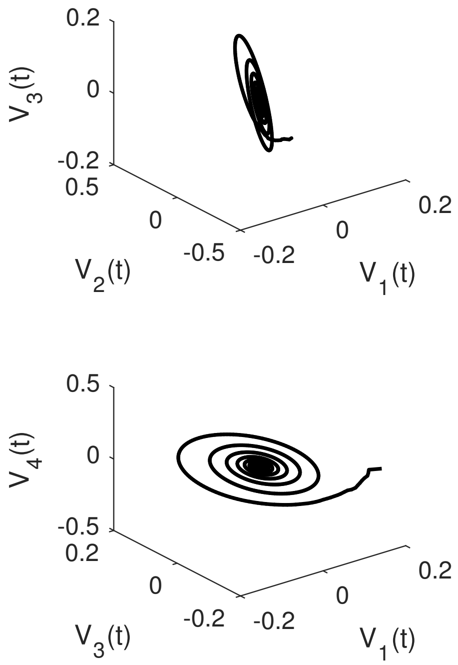

Figure 16. The portraits of FONTINN (16) with $\iota = 0.85 < \iota_0 = 1.0135$.

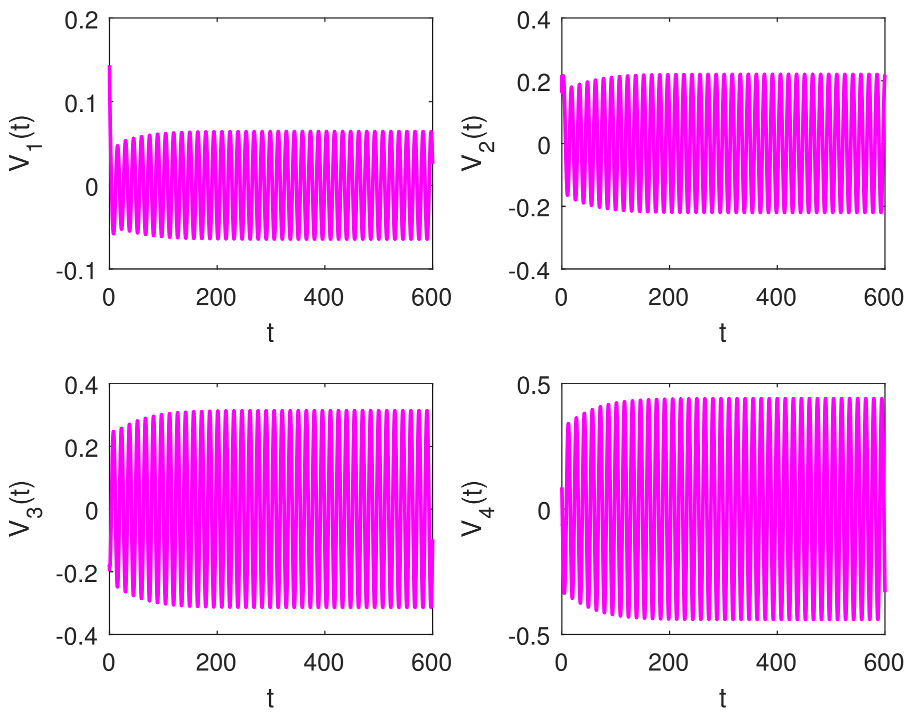

Figure 17. Trajectories of FONTINN (16) with $\iota = 1.1 > \iota_0 = 1.0135$.

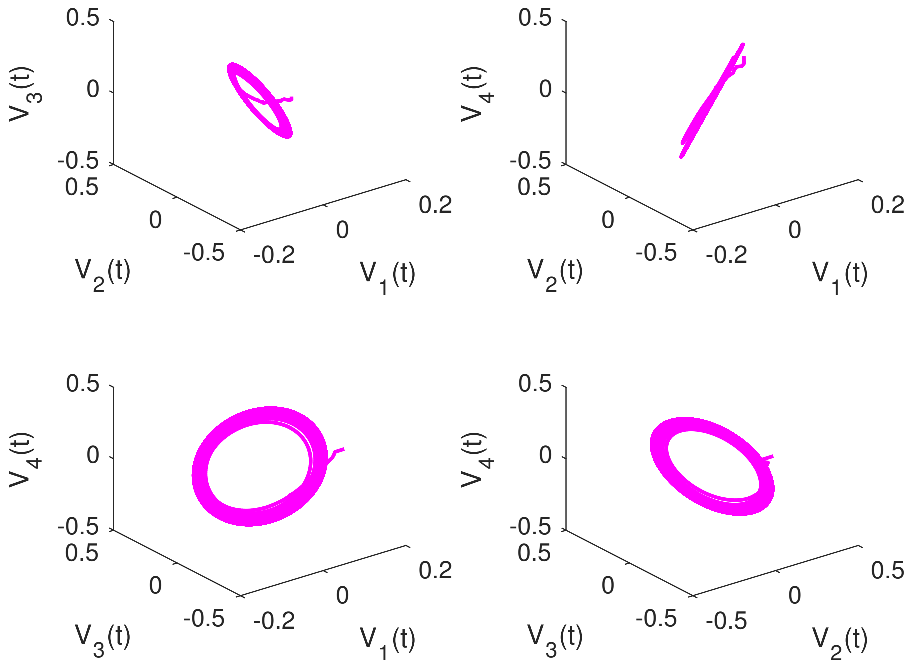

Figure 18. The portraits of FONTINN (16) with $\iota = 1.1 > \iota_0 = 1.0135$.

6. Conclusions

This article has elaborated on the dynamic characteristics of the four-neuron fractional-order neutral-type inertial neural network. Detailed discussions have been conducted on the stability of the system under two different scenarios, one was that the system does not have time delay, and the other was that the system have time delay. Important bifurcation results have been obtained in the end. Through two numerical simulations, the precise bifurcation points have been figured out. The time history and phase diagrams of the system have been drawn. The correctness of the conclusions drawn has been confirmed. Simultaneously, we also have found that time delay not only can affect the stability of the system, but also fractional order changes have the function of delaying and advancing the occurrence of system bifurcations. Therefore, we have analyzed the impact of changing only one fractional order on the bifurcation results of the system and proved the above findings. Finally, we have compared the original simulation with integer order systems and found that the bifurcation points of integer order systems are relatively small. It has indirectly revealed that fractional-order neural networks improved the performance stability of the system better.

Some valuable research directions are worthy of further exploration:

(1) Based on this paper, we find that fractional order has important influence on the stability of fractional-order neutral-type inertial neural network. Thereby, fractional order-induced bifurcations will be studied.
(2) If the parameters of coefficients involve timed delays, how to decide the bifurcation conditions of fractional-order neutral-type inertial neural network?
(3) Discrete fractional-order neural networks have become an active research topic. How to establish the conditions of bifurcations of these neural networks?

Author Contributions

C.H.: Writing-original draft; H.C.: Methodology; J.C.: Supervision; H.L.: Funding acquisition, Resources. All authors have read and agreed to the published version of the manuscript.

Funding

This work received funding from the National Natural Science Foundation of China under Grant No. 12571583.

Institutional Review Board Statement

Not applicable.

Informed Consent Statement

Not applicable.

Data Availability Statement

No data was used for the research described in the article.

Conflicts of Interest

The authors declare no conflict of interest.

Use of AI and AI-Assisted Technologies

No AI tools were utilized for this paper.

References

1. Sawar, S.; Hussain, S.; Ayaz, M. Secure Image Transmission Using Fractional Variable Order Memristive Hyperchaotic System with Nonlinear Synchronization. *Adv. Anal. Appl. Math.* **2025**, *2*, 32–43.
2. Shakeel, M.; Liu, X.; Tang, M.; et al. Synchronization and image encryption via Caputo-Hadamard fractional-order memristive neural networks with time-varying delay. *Commun. Nonlinear Sci. Numer. Simul.* **2026**, *161*, 1101203.
3. Li, J.; Shi, P.; Wang, J.; et al. Dynamically optimized fractional-order model predictive control for high-precision spacecraft proximity operations. *Aerosp. Sci. Technol.* **2026**, *176*, 112505.
4. Abbas, N.; Hao, L. Intelligent hybrid neural network-reinforcement learning framework for fault-tolerant formation control. *Aerosp. Sci. Technol.* **2026**, *171*, 111582.
5. Nguyen, L.; Tran, K. Explainable artificial intelligence in uncertainty quantification of functionally graded triply periodic minimal surface nanoplates via nonlocal moving Kriging meshfree method and Bayesian neural networks. *Comput. Struct.* **2026**, *326*, 108217.
6. Man, T.; Osipov, V.; Zhukova, N.; et al. Neural networks for intelligent multilevel control of artificial and natural objects based on data fusion: A survey. *Inf. Fusion* **2024**, *110*, 102427.
7. Gerard, D.; Deepak, S.; Ishdutt, T.; et al. An artificially intelligent approach for automatic speech processing based on triune ontology and adaptive tribonacci deep neural networks. *Comput. Electr. Eng.* **2022**, *98*, 107736.
8. Cheng, H.; Yang, Y.; Shi, J.; et al. Comparison of automated deep neural network against manual sleep stage scoring in clinical data. *Comput. Biol. Med.* **2024**, *179*, 108855.
9. Wang, Y. Organic integration of ideological and political education and entrepreneurship education based on artificial neural network. *Learn. Motiv.* **2023**, *84*, 101933.
10. Zheng, Y.; Wang, J.; Wang, H.; et al. Parametric design of curved hydrocyclone and its optimization based on artificial neural networks prediction. *Sep. Purif. Technol.* **2025**, *353*, 128445.
11. Lakhani, P.; Alankar, B.; Ashraf, S.S.; et al. A novel cloud architecture approach to detect network intrusions using an enhanced artificial neural network. *Int. J. Inf. Technol.* **2024**, *16*, 3929–3939.
12. Wu, X.; Mei, J.; Xu, Y.; et al. Stack performance classification and fault diagnosis optimization of solid oxide fuel cell system based on bayesian artificial neural network and feature selection. *J. Power Sources* **2024**, *620*, 235198.
13. Ben Hmida, R.; Bahloul, R.; Richard, F.; et al. Identification and Identifiability Analysis of Material Parameters Using Hybrid Optimization Algorithms and Optimized Artificial Neural Networks. In Proceedings of the 10th Conference on Design and Modeling of Mechanical Systems, CMSM'2023, Hammamet, Tunisia, 18–20 December 2023; Volume 2: Materials Engineering and Manufacturing; Vol. 28, pp. 77–85.
14. Yu, E.; Du, J.; Yang, X.; et al., Explainable artificial intelligence and domain adaptation for predicting HIV infection with graph neural networks. *Ann. Med.* **2024**, *56*, 2407063.
15. Wang, H.; Huang, C.; Li, S.; et al. Bifurcation detections of a fractional-order neural network involving three delays. *J. Appl. Math. Comput.* **2024**, *70*, 579–599.
16. Huang, C.; Li, H.; Chen, X.; et al. Bifurcations emerging from different delays in a fractional-order perdator-pery model. *Fractals* **2021**, *29*, 2150040.
17. Kumar, R.; Das, S. Exponential stability of inertial BAM neural network with time-varying impulses and mixed time-varying delays via matrix measure approach. *Commun. Nonlinear Sci. Numer. Simul.* **2020**, *81*, 105016.
18. Wheeler, D.; Schieve, W. Stability and chaos in an inertial two-neuron system. *Physica D* **1997**, *105*, 267–284.
19. Fei, J.; Ren, S.; Zheng, C.; et al. Aperiodically intermittent quantized control-based exponential synchronization of quaternion-valued inertial neural networks. *Neural Netw.* **2024**, *180*, 106669.
20. Kowsalya, P.; Kathiresan, S.; Kashkynbayev, A.; et al. Fixed-time synchronization of delayed multiple inertial neural network with reaction-diffusion terms under cyber-hysical attacks using distributed control and its application to multi-image encryption. *Neural Netw.* **2024**, *180*, 106743.

21. Kowsalya, P.; Mohanrasu, S.; Kashkynbayev, A.; et al. Fixed-time synchronization of Inertial Cohen-Grossberg Neural Networks with state dependent delayed impulse control and its application to multi-image encryption. *Chaos Solitons Fract.* **2024**, *181*, 114693.
22. Huang, C.; Wang, H.; Gao, J.; et al. Delay-dependent bifurcation conditions in a fractional-order inertial BAM neural network. *Chaos Solitons Fract.* **2024**, *185*, 115106.
23. Liu, L.; Bao, H.; Gao, J. Adaptive finite-time synchronization of quaternion-valued inertial neural networks with mixed delays under quantized event-triggered impulsive strategy. *J. Frankl. Inst.* **2024**, *361*, 107020.
24. Wang, H.; Gu, Y.; Zhang, X.; et al. Stability and synchronization of fractional-order reaction-iffusion inertial time-delayed neural networks with parameters perturbation. *Neural Netw.* **2024**, *179*, 106564.
25. Gan, B.; Chen, H.; Xu, B.; et al. A norm stability condition of neutral-type Cohen-Grossberg neural networks with multiple time delays. *Chaos Solitons Fract.* **2023**, *175*, 113958.
26. Wang, X.; Lan, J.; Yang, X.; et al. Global robust exponential synchronization of neutral-type interval Cohen-rossberg neural networks with mixed time delays. *Inf. Sci.* **2024**, *676*, 120806.
27. Song, Q.; Yang, L.; Liu, Y.; et al. Stability of quaternion-valued neutral-type neural networks with leakage delay and proportional delays. *Neurocomputing* **2023**, *521*, 191–198.
28. Wang, W.; Chen, W. New study on neutral-type inertial BAM neural networks via the characteristic method. *J. Math. Anal. Appl.* **2026**, *557*, 130325.
29. Fang, W.; Xie, T.; Zhu, Q.; et al. Fixed time stabilization of stochastic neutral-type fuzzy inertial neural network with mixed delays. *Fuzzy Sets Syst.* **2025**, *520*, 109566.
30. Huang, C.; Wang, H.; Cao, J.; et al. Multi-parametric bifurcations of a fractional neural network with multiple delays and inertial terms. *Neural Netw.* **2026**, *197*, 108456.
31. Jia, S.; Zhou L. Fixed-time stabilization of fuzzy neutral-type inertial neural networks with proportional delays. *ISA Trans.* **2024**, *144*, 167–175.
32. Duan, L.; Li, J. Global exponential bipartite synchronization for neutral memristive inertial coupling mixed time-varying delays neural networks with antagonistic interactions. *Commun. Nonlinear Sci. Numer. Simul.* **2023**, *119*, 107071.
33. Huang, C.; Liu, H.; Wang, H.; et al. Dynamical Bifurcations of a Fractional-Order BAM Neural Network: Nonidentical Neutral Delays. *IEEE Trans. Netw. Sci. Eng.* **2024**, *11*, 1668–1679.
34. Podlubny, I. *Fractional Differential Equations*; Academic Press: New York, NY, USA, 1999.
35. Deng, W.; Li, C.; Lü, J. Stability analysis of linear fractional differential system with multiple time delays. *Nonlinear Dyn.* **2007**, *48*, 409–416.